

D.S. BAER[✉]
J.B. PAUL
M. GUPTA
A. O'KEEFE

Sensitive absorption measurements in the near-infrared region using off-axis integrated-cavity-output spectroscopy

Los Gatos Research, 67 East Evelyn Avenue, Suite 3, Mountain View, CA 94041-1518, USA

Received: 6 May 2002/Revised version: 31 May 2002
Published online: 2 September 2002 • © Springer-Verlag 2002

ABSTRACT A novel instrument that employs a high-finesse optical cavity as an absorption cell has been developed for sensitive measurements of gas mixing ratios using near-infrared diode lasers and absorption-spectroscopy techniques. The instrument employs an off-axis trajectory of the laser beam through the cell to yield an effective optical path length of several kilometers without significant unwanted effects due to cavity resonances. As a result, a minimum detectable absorption of approximately 1.4×10^{-5} over an effective optical path of 4.2 km was obtained in a 1.1-Hz detection bandwidth to yield a detection sensitivity of approximately $3.1 \times 10^{-11} \text{ cm}^{-1} \text{ Hz}^{-1/2}$. The instrument has been used for sensitive measurements of CO, CH₄, C₂H₂ and NH₃.

PACS 42.79.P; 78.40.M; 33.55.A

1 Introduction

Sensitive and accurate measurements of trace gases using laser-based diagnostics may serve to characterize global climate change due to anthropogenic and biogenic effects [1–6], monitor and control combustion and other industrial processes [7, 8], and improve the understanding of semiconductor manufacturing processes [9].

Various methods have been developed to achieve sensitive measurements using laser diagnostics techniques including direct-absorption spectroscopy using long-path multipass cells [10], wavelength- (and frequency-) modulation spectroscopy [11], cavity-ringdown spectroscopy [12], cavity-enhanced absorption spectroscopy [13], and integrated-cavity-output spectroscopy (ICOS) [14], and recently, off-axis integrated-cavity-output spectroscopy (off-axis ICOS) [15].

ICOS allows narrowband, continuous-wave lasers to be used in conjunction with optical cavities in a simple and effective manner [16, 17]. The absorption signal is obtained through the temporal integration of the laser intensity trans-

mitted through the cavity in the same fashion as in conventional absorption measurements. The absorption due to the medium inside the cavity is determined from the cavity output (i.e. laser transmission), which is a function of the mirror reflectivity as well as scattering and absorption losses between the mirrors [17]. The conventional ICOS approach requires a relatively simple set-up because it does not require the laser to be optically mode-matched to the cavity. Indeed, ICOS is based on systematically disrupting the cavity resonances to yield the frequency-averaged cavity transmission, which is sensitive to the round-trip laser intensity loss experienced by the circulating beam inside the cavity. Off-axis ICOS is a new variation of ICOS that is sensitive, robust and simple to implement. For example, an off-axis ICOS instrument using a quantum-cascade laser operating near 8 microns was designed and recently flown on a NASA WB-57 aircraft to monitor trace gases in the stratosphere [18].

In this work, we present quantitative measurements using a novel instrument based on the off-axis ICOS technique with room-temperature semiconductor diode lasers operating in the 1.5–1.65 micron region. The instrument is used for measurements of CO, CH₄, NH₃ and C₂H₂ mixing ratios to demonstrate the potential for a range of applications, including atmospheric sensing and industrial process monitoring.

2 Technical approach

The basis for off-axis ICOS has been presented previously [15]. In brief, the technique is based on directing the laser beam off axis with respect to the cavity. Off-axis paths through optical cavities are well understood [20, 21] and, in effect, spatially separate the multiple reflections within the cavity until the light retraces its path through the cavity. This so-called “re-entrant condition” is dictated by the cavity geometry [15].

The transmitted laser intensity (I) through an empty cavity may be expressed by [15]:

$$I = \frac{I_L C_p T}{2(1-R)} (1 - \exp(-t/\tau)), \quad \tau = \frac{L/c}{1-R}, \quad (1)$$

✉ Fax: +1-650/965-7074, E-mail: d.baer@lgrinc.com

where I_L is the incident (or reference) laser intensity, C_p is a cavity coupling parameter, R and T are the mirror intensity reflection and transmission coefficients, τ is the characteristic cavity (ringdown) decay time, L is the distance between the mirrors, and c is the speed of light. The coupling parameter C_p depends on geometrical factors and the mode quality of the light source and has a value between 0 and 1.

After the laser beam enters the cavity, the intensity inside the cavity increases with the characteristic time constant τ . After sufficient laser power is leaving the cavity, the laser can be interrupted to observe the ringdown decay. Since the laser is continuously coupled into the cavity, the characteristic decay time τ may be recorded, whenever necessary, with the laser tuned to a non-absorbing wavelength i.e. 'off line', or in an empty cavity to monitor the effective optical path length in the cavity $L_{\text{eff}} = L/(1 - R)$.

With an absorbing gas between the mirrors, R is replaced by R' , given by:

$$R' = R \exp(-\alpha(\nu)) \quad (2)$$

where $\alpha(\nu)$ represents the optical depth (at frequency ν) of the gas over the cavity length. Comparing (2) with the Beer–Lambert absorption formula for a single pass ($I/I_0 = \exp(-\alpha(\nu))$) through the cavity reveals that $I/I_0 = R'/R$. Thus (1) and (2) indicate that essential absorption information is contained in the *steady-state* cavity-output intensity. From these equations, the change in steady-state cavity output ($\Delta I = I_L - I$) due to the presence of an absorbing species may be expressed as:

$$\frac{\Delta I}{I_0} = \frac{GA}{1 + GA} \quad (3)$$

where A is the single-pass absorption [$A = 1 - \exp(-\alpha(\nu))$] and $G = R/(1 - R)$.

The mole fraction of the probed species may be determined from the measured spectra integrated over the entire absorption feature, together with the measured temperature and total pressure in the cell, effective optical path length, and line strength(s) of the target species [7].

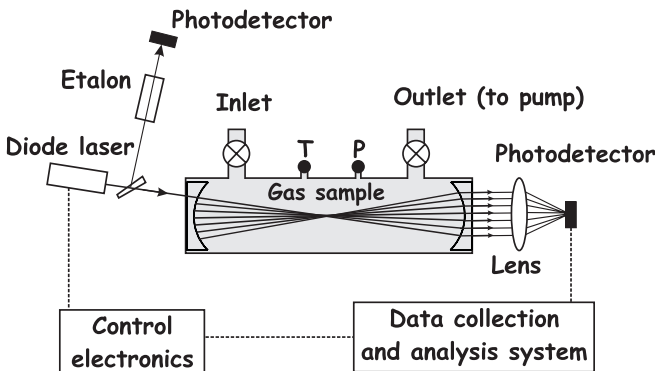


FIGURE 1 Schematic diagram of the instrument based on off-axis ICOS for high-sensitivity absorption measurements in the near-infrared region. The measurement cell is comprised of a cylindrical tube sealed by a pair of high-reflectivity mirrors. The relative laser wavelength is measured by recording the laser transmission through a solid (FSR = 2.00 GHz) etalon. The beams propagating out of the cell through the left-side cavity mirror have been omitted for clarity

3 Experimental

Figure 1 illustrates the experimental set-up employed for the off-axis ICOS measurements using semiconductor diode lasers mounted in butterfly packages. For the present work, the optical cavity consisted of two 1-m-radius-of-curvature, 2-inch-diameter mirrors. The measured loss of the cavity mirrors ($1 - R$) ranged from 130 ppm at 1500 nm to 410 ppm at 1650 nm. The measurement cell consisted of a stainless-steel tube sealed by a pair of high-reflectivity mirrors mounted in stainless-steel flanges, which could be adjusted to optimize the cavity alignment. The distance between the mirrors could be varied coarsely by using 10-cm-long stainless-steel cylindrical tubes as spacers. The nominal spacing between the mirrors was about 80 cm, but ranged from about 60 cm to 90 cm during the course of this work. An aspheric lens and steering mirror (not shown) were used to loosely focus the beam into the cavity at an acute angle with respect to the cavity axis, so that a Lissajous spot pattern was generated on the cavity mirrors.

The wavelengths of the diode lasers were tuned by supplying a saw-tooth current ramp to the laser current source while holding the diode-laser case temperature constant. A portion of the beam was directed through a fused-silica etalon (2-GHz free spectral range) using a wedge beam splitter to allow determination of the relative wavelength as the laser was tuned over the probed absorption feature. The laser wavelength tuning rate was set at a value much less than the characteristic cavity frequency $f_{\text{cavity}} = 1/(2\pi\tau)$, which describes the amplitude response of the laser beam propagating through the cavity, see (1).

The beams exiting the cavity and etalon were focused by aspheric lenses onto individual amplified InGaAs photodetectors, which converted the laser intensities to voltage signals. The voltage signals were then digitized using a 16-bit A/D board inside a personal computer. A pressure gauge was used to monitor total gas pressure in the cell.

Cavity ringdown measurements were recorded to determine the effective mirror loss ($1 - R$), and thus effective optical path length in the cavity at each wavelength. Figure 2 (bottom frame) shows a typical ringdown measurement obtained by rapidly switching the diode-laser current below the threshold (at $t = 0$). A measured decay time of $\tau = 22.5 \mu\text{s}$ corresponded to a mirror loss ($1 - R$) of 130 ppm and an effective optical path length of 6770 m for a 0.88-m-long cell. The top frame shows the residual or fractional difference between the normalized data and least-squares-fit to an exponential decay. The good agreement between the data and the fit over eight time constants indicates that the cavity decay may be described accurately by a single-exponential time constant. The slight 'ringing' or non-exponential behavior within the first 5–10 μs after the start of the decay was due to the finite frequency response (1-MHz electrical bandwidth) of the laser current source.

Measurements of cavity ringdown decay were recorded regularly to confirm the integrity of the cavity mirrors in the measurement cell. During the present investigation, which lasted about 60 days, we did not observe variations in mirror loss at any of the probed wavelengths.

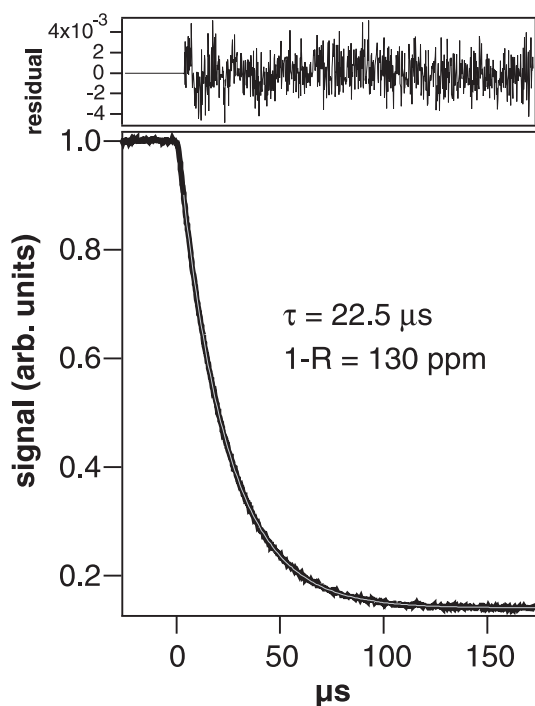


FIGURE 2 (*bottom frame*) Example cavity-ringdown decay measurement recorded in an 88-cm-long cell used to determine mirror loss ($1 - R$) at a given wavelength, recorded by rapidly switching the diode-laser current below threshold. (*top frame*) The residual or fractional difference between the normalized data and least-squares fit to a single-exponential decay over eight time constants

4 Measurements

Table 1 lists the species and corresponding transitions probed in the present work. The individual transitions were selected based on their relative strength and spectral isolation in typical industrial and atmospheric flows.

Figure 3 presents measurements of CO, CO₂ and H₂O absorption in local ambient air (Mountain View, California), unfiltered for particulates, in a 70-cm-long cell (total pressure = 75 Torr, temperature = 298 K), obtained by tuning a diode laser over a 20-GHz region near 1565 nm at a 100-Hz rate over a total measurement interval of 100 s (10 000-sweep average). The bottom frame shows the measured single-pass absorption through the cell and the calculated spectra (displaced vertically by 50×10^{-9} for clarity) from HITRAN96 [21] (at 298 K). The mole fractions of CO₂ (440 ppmv) and CO (500 ppbv) were determined from the measured spectra. The observed H₂O absorption feature near 6390.5 cm^{-1} is not listed in HITRAN96. The top frame displays the residual, the difference between the data and individual Voigt fits to the measured lineshapes. These features would be difficult to ob-

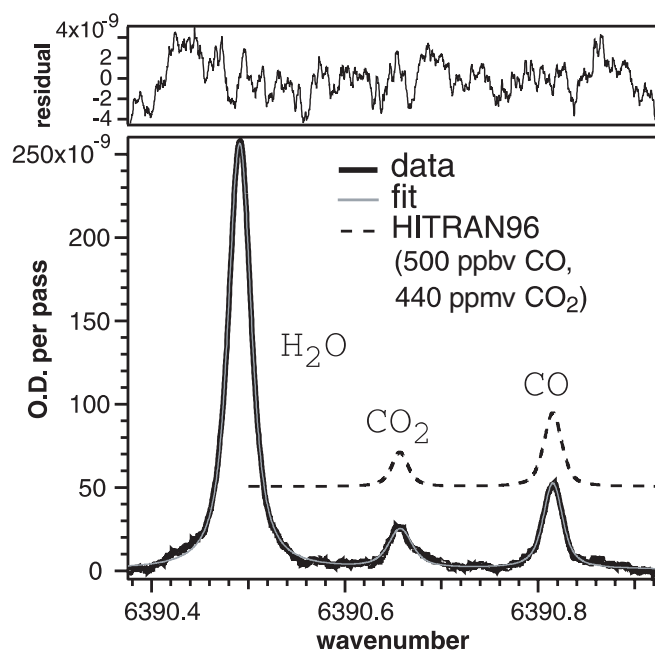


FIGURE 3 Absorption measurements of CO, CO₂ and H₂O in ambient air (Mountain View, California) obtained by tuning a diode laser over a 20-GHz region near 1565 nm at a 100-Hz rate. The *bottom frame* shows the measured single-pass absorption through the cell and the calculated spectra (displaced vertically by 50×10^{-9} for clarity) from HITRAN96 (at 298 K). The mole fractions of CO₂ (440 ppmv) and CO (500 ppbv) were determined from the measured spectra, path length, gas temperature and total pressure in the cell, and tabulated parameters in the HITRAN96 database. The observed H₂O absorption feature is not listed in HITRAN2000. The *top frame* displays the residual, the difference between the data and individual Voigt fits to the measured lineshapes

serve using standard absorption techniques using multi-pass cells.

Figure 4 shows a CO absorption measurement (total pressure = 75 Torr, temperature = 298 K) in local ambient air obtained by tuning a diode laser over the CO (R(12), 3 ν band) transition near 1564.75 nm at a 200-Hz rate for a 50-s integration time (10 000-sweep average). At this wavelength, the measured cavity decay time ($\sim 14 \mu\text{s}$) and base length ($\sim 70 \text{ cm}$) yielded an effective optical path of approximately 4200 m. The CO mole fraction (500 ppbv) was determined from the measured absorption, gas temperature and total pressure in the cell, effective optical path length and tabulated parameters in HITRAN96. For the present measurements, the CO detection limit was approximately 36 ppbv ($S/N \sim 3$). The absorption feature observed in the wing of the CO transition at -300 MHz , presumably due to H₂O, is not included in HITRAN2000.

Similarly, Fig. 5 presents a measurement of ambient CH₄ absorption in a sample of local air (total pressure $\sim 100 \text{ Torr}$, 298 K) obtained by wavelength tuning a diode

Gas	Wavelength (nm)	Transition	Reference
CO	1564.746	R(12), 3 ν band	[21]
C ₂ H ₂	1531.588	P(11), $\nu_1 + \nu_3$ band	[22]
NH ₃	1531.684	($J' = 4, K' = 2; J'' = 5, K'' = 3, \sigma = a$), $\nu_1 + \nu_3$ band	[23]
CH ₄	1653.723	R(3), 2 ν_3 band	[21]

TABLE 1 Species and corresponding transitions probed in the present work

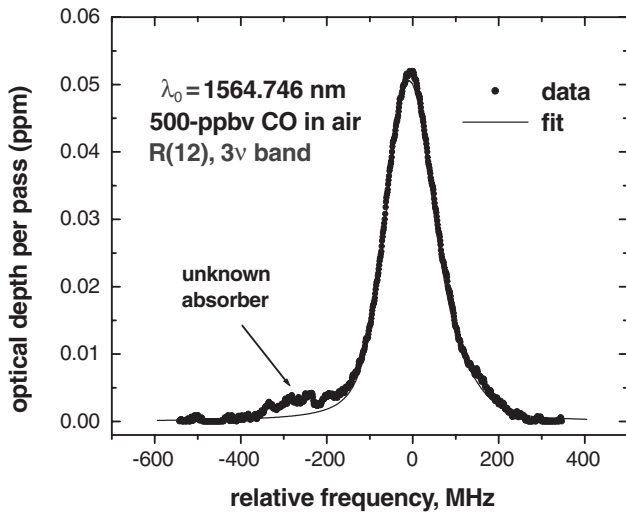


FIGURE 4 Absorption measurement of CO in ambient air (Mountain View, California) obtained by tuning a diode laser over the CO (R12, 3ν band) transition near 1564.75 nm at a 200-Hz rate for a 50-s integration time (10000-sweep average). The CO mole fraction (500 ppbv) was determined from the measured absorption, effective optical path length, gas temperature and total pressure in the cell and parameters in the HITRAN96 database. The CO detection limit was approximately 36 ppbv ($S/N \sim 3$). The absorption feature observed in the wing of the CO transition at -300 MHz, presumably due to H_2O , is not included in HITRAN2000

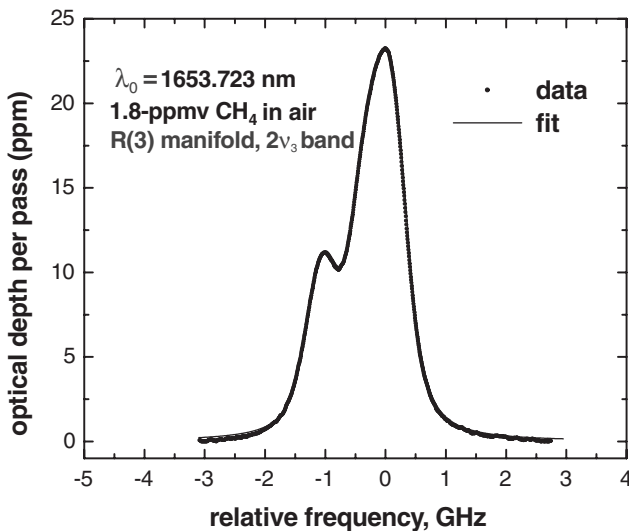


FIGURE 5 Absorption measurement of CH_4 in ambient air (Mountain View, California) obtained by tuning a diode laser over three overlapping CH_4 transitions (R(3) manifold, $2\nu_3$ band) near 1653.7 nm at a 600-Hz rate for a 1-s integration time (600-sweep average). The CH_4 mole fraction (1.8 ppmv) was determined from the measured absorption, path length, gas temperature and total pressure in the cell and tabulated parameters in the HITRAN96 database. The CH_4 detection limit ($S/N \sim 3$) was approximately 1 ppbv in a 1-s measurement time

laser across three overlapping lines near 1653.7 nm (R(3) manifold, $2\nu_3$ band) at a 600-Hz rate in a 1-s integration time (600-sweep average). At this wavelength, the measured cavity decay time ($\sim 7 \mu s$) and base length (~ 88 cm) yielded an effective optical path of approximately 2100 m. The CH_4 mole fraction (~ 1.80 ppmv) was determined from the measured optical depth, path length, gas temperature and total pressure, and parameters in HITRAN96. The CH_4 detection limit ($S/N = 3$) was approximately 1 ppbv.

For measurements of NH_3 absorption, 50-ppmv NH_3 in N_2 from a cylinder (Matheson) was inserted in the cell to a pressure of 1 Torr and mixed with 99 Torr of room air to yield a 5-ppmv mixture of NH_3 at a total pressure of 100 Torr. Figure 6 presents absorption measurements of NH_3 (5 ppmv in air) obtained by tuning a diode laser over the NH_3 transition near 1531.6 nm at a 100-Hz rate for a 1-s integration time (100-sweep average). The measured cavity decay time at the probed wavelength 1532 nm ($\sim 16.8 \mu s$) and base length (~ 70 cm) yielded an effective optical path of approximately 5035 m. The NH_3 detection limit was approximately 2 ppbv ($S/N \sim 3$) in a 1-s measurement time.

Figure 7 shows a C_2H_2 absorption measurement (100-ppbv in N_2 at 50-Torr total pressure) obtained by wave-

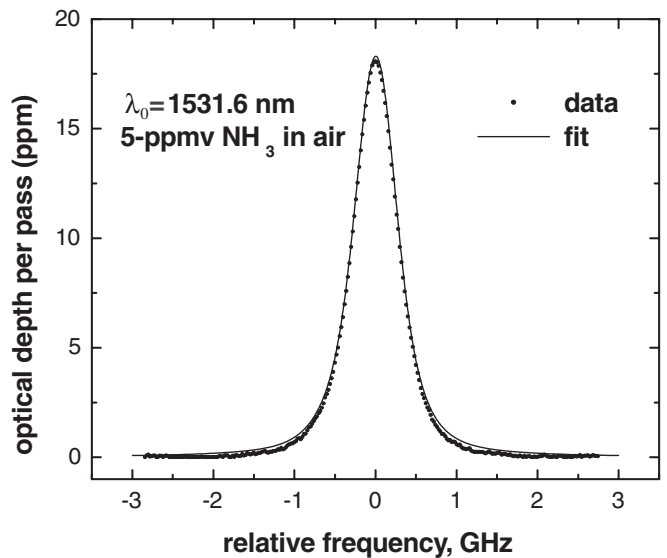


FIGURE 6 Absorption measurement of NH_3 (5 ppmv in air) obtained by tuning a diode laser over the NH_3 transition near 1531.6 nm at a 100-Hz rate for a 1-s integration time (100-sweep average). The NH_3 detection limit was approximately 2 ppbv ($S/N \sim 3$)

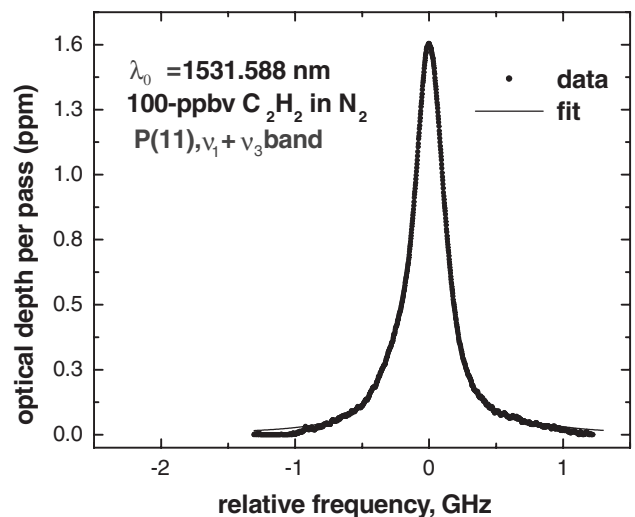


FIGURE 7 Absorption measurement of C_2H_2 (100-ppbv in N_2) obtained by tuning a diode laser over the P(11) transition ($\nu_1 + \nu_3$ band) near 1531.6 nm at a 500-Hz rate for a 1-s integration time (500-sweep average). The C_2H_2 detection limit was approximately 0.3 ppbv ($S/N \sim 3$)

length tuning a DFB diode laser across the P(11) transition ($\nu_1 + \nu_3$ band) [22] near 1532 nm at a 500-Hz rate in a 1-s integration time (500-sweep average). The C_2H_2 detection limit ($S/N \sim 3$) was approximately 0.3 ppbv for these conditions. Since the ambient mixing ratio of C_2H_2 is approximately 0.1 ppbv [21], these results suggest that the present measurement strategy may be applied for atmospheric monitoring with increased signal averaging. For measurements in industrial process flows, such as those in olefin plants where C_2H_2 may be a contaminant, an effective instrument would have to account for absorption features due to other hydrocarbons (e.g. C_2H_4 and C_3H_4) in the probed flow that interfere spectrally with the probed C_2H_2 transition.

The noise equivalent absorption sensitivity at a given wavelength was determined from the minimum detectable absorption, effective optical path length in the cell, and detection bandwidth. For these measurements, the detection bandwidth corresponded to the cavity bandwidth [$f_{\text{cavity}} = 1/(2\pi\tau)$] divided by the number of sweeps averaged. As an example, for the CO measurements near 1565 nm, a minimum detectable absorption of 1.4×10^{-5} in a detection bandwidth of 1.1 Hz ($f_{\text{cavity}} = 11$ kHz, 10^4 -sweep average) over an effective optical path length of 4200 m yielded a noise equivalent absorption sensitivity of approximately $3.1 \times 10^{-11} \text{ cm}^{-1} \text{ Hz}^{-1/2}$. Not surprisingly, the minimum detectable absorption was limited by residual optical interference effects in the cell.

The goal of the present work was to demonstrate the potential of the instrument to provide quantitative measurements at ppbv-levels from absorption spectra recorded in the near-infrared region. Further work is currently underway at Los Gatos Research to establish the long-term robustness and to characterize the precision and accuracy of the instrument from replicate and Allen variance measurements.

5 Conclusions

A novel instrument based on off-axis integrated cavity output spectroscopy and room-temperature near-infrared diode lasers has been applied for measurements of several species. The instrument effectively combines the advantages of high-finesse optical cavities with the simplicity of direct-absorption-spectroscopy techniques to yield

fast, sensitive and absolute gas mole-fraction measurements. The system demonstrated a minimum detectable absorption of approximately 1.4×10^{-5} in a cell with an effective optical path length of 4200 m in a 1.1-Hz detection bandwidth to yield a detection sensitivity of approximately $3.1 \times 10^{-11} \text{ cm}^{-1} \text{ Hz}^{-1/2}$. Uses for the instrument include those applications requiring sensitive gas measurements in a compact and inexpensive package operating at room temperature.

REFERENCES

- 1 G. Durry: Appl. Opt. **41**, 424 (2002)
- 2 A.C. Stanton, D.S. Bomse, J.A. Silver, D.C. Hovde, D.B. Oh: 'Measurement of Atmospheric Species by Mid-Infrared and Near-Infrared Tunable Diode Laser Absorption'. In: Monitoring of Gaseous Pollutants by Tunable Diode Lasers: Proc. Int. Symp. Freiburg, Germany, 17–18 October 1991, ed. by R. Grisar, H. Boettner, M. Tacke, G. Restelli (Kluwer Academic Publishers, Dordrecht 1992) pp. 31–40
- 3 D.C. Scott et al.: Appl. Opt. **38**, 4609 (1999)
- 4 F.G.C. Bijnen et al.: Appl. Opt. **35**, 5357 (1996)
- 5 A. Fried et al.: Appl. Phys. B **67**, 317 (1998)
- 6 C.E. Kolb et al.: 'Recent Advances in Spectroscopic Instrumentation for Measuring Stable Gases in the Natural Environment'. In: *Methods in Ecology: Biogenic Trace Gases: Measuring Emissions from Soil and Water*, ed. by A. Matson, R.C. Harriss (Blackwell Scientific Publishers Ltd., Oxford 1995) pp. 259–290
- 7 R.M. Mihalcea et al.: Meas. Sci. Technol. **9**, 327 (1998)
- 8 E.R. Furlong et al.: Proceedings of the Twenty-Seventh Symposium (International) on Combustion. The Combustion Institute, Pittsburgh (USA), 103–111 (1998)
- 9 S.I. Chou et al.: J. Vac. Sci. Technol. A **19**, 477 (2001)
- 10 J.B. McManus et al.: Appl. Opt. **34**, 3336 (1995)
- 11 J.A. Silver: Appl. Opt. **31**, 707 (1992)
- 12 A. O'Keefe, D.A.G. Deacon: Rev. Sci. Instrum. **59**, 2544 (1988)
- 13 R. Engeln et al.: Rev. Sci. Instrum. **69**, 3763 (1998)
- 14 A. O'Keefe: Chem. Phys. Lett. **293**, 331 (1998)
- 15 J.B. Paul et al.: Appl. Opt. **40**, 4904 (2001)
- 16 A. O'Keefe: Chem. Phys. Lett. **293**, 331 (1998)
- 17 A. O'Keefe et al.: Chem. Phys. Lett. **307**, 343 (1999)
- 18 J.B. Paul et al.: SPIE Proc. **4577**, 1 (2001)
- 19 D.R. Herriott et al.: Appl. Opt. **3**, 523 (1964)
- 20 D.R. Herriott, H.J. Schulte: Appl. Opt. **4**, 883 (1965)
- 21 L.S. Rothman et al.: J. Quant. Spectrosc. Radiat. Transfer **60**, 665 (1998)
- 22 S.L. Gilbert, W.L. Swann: 'Acetylene $^{12}C_2H_2$ absorption reference for 1510 nm to 1540 nm wavelength calibration – SRM 2517a'. In: *NIST Special Publication*, 2001 edn., pp. 260–133
- 23 M.E. Webber et al.: Appl. Opt. **40**, 2031 (2001)